IEEE Photonics Journal
An IEEE Photonics Society Publication

Open Access

Memory-Based Codes for Uniform Illumination in MIMO VLC

Volume 12, Number 2, April 2020

Thummaluri Uday, ***Student Member, IEEE***
Abhinav Kumar, ***Member, IEEE***
Lakshmi Natarajan, ***Member, IEEE***

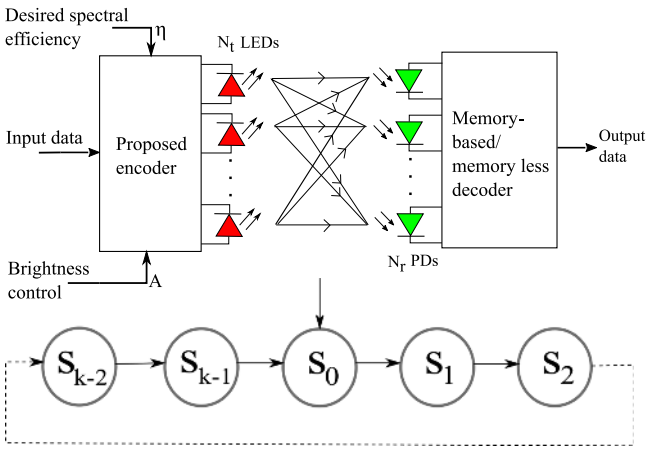

DOI: 10.1109/JPHOT.2020.2981008

Memory-Based Codes for Uniform Illumination in MIMO VLC

Thummaluri Uday, *Student Member, IEEE*,
Abhinav Kumar, *Member, IEEE*,
and Lakshmi Natarajan, *Member, IEEE*

Department of Electrical Engineering, Indian Institute of Technology Hyderabad, Telangana 502285, India

DOI:10.1109/JPHOT.2020.2981008

Manuscript received February 21, 2020; accepted March 10, 2020. Date of publication March 16, 2020; date of current version April 16, 2020. This work was supported by the Department of Science and Technology under Grant TMD/CERI/BEE/2016/059(G). Corresponding author: Uday Thummaluri (e-mail: ee18resch11005@iith.ac.in).

Abstract: Light emitting diode (LED) based indoor multiple input multiple output visible light communication system has LEDs placed at various positions in the room which are simultaneously used for illumination and communications. In such a system, there should be no human perceivable fluctuations in the intensity of the individual LEDs to avoid user discomfort. In order to achieve the uniformity in illumination, we propose codes under the constraints of constant total transmit power per symbol and constant average transmit power for each individual LED. We show the performance of the proposed codes in terms of various metrics like bit error rate (BER), consistency in illumination, and spectral efficiency with suitable expressions. We also numerically analyze the impact of channel state information (CSI) on BER performance by assuming perfect CSI is not always available but periodically updated at the receiver.

Index Terms: Bit error rate, multiple input multiple output, spectral efficiency, visible light communications.

1. Introduction

Multiple input multiple output (MIMO) visible light communication (VLC) systems typically use light emitting diodes (LEDs) as the transmit antennas because of the numerous advantages that LEDs have over the traditional lighting sources [1]. In indoor environment, such LED-based MIMO VLC systems can be used for simultaneous illumination and communications. For such a system, users shouldn't perceive changes in the light intensity while the data is being transmitted to avoid discomfort to the eyes. Hence, we need to maintain uniformity in illumination over time at system level, i.e., considering all the LEDs and also at individual LED level. Maintaining this uniform illumination at individual LED level is important as a stationary or moving user should not perceive different illumination from each LED. Several coding schemes have been proposed for MIMO VLC systems such as space shift keying (SSK) [2], generalized space shift keying (GSSK) [3], spatial multiplexing (SMP) [4], spatial modulation (SM) [5], generalized spatial modulation (GSM) [6], dual-LED complex modulation (DCM) [7], and quad-LED complex modulation (QCM) [8].

In SSK and GSSK, the number of active LEDs per channel use are fixed and each of these active LEDs has the same transmit power per channel use ensuring uniform illumination at

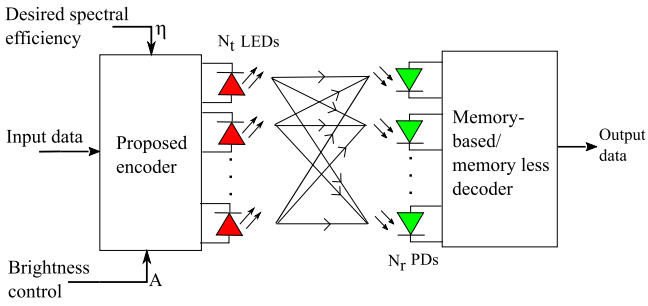

Fig. 1. System model.

system level across time slots. However, these schemes do not ensure uniform illumination at individual LED level. For example, consider a 4 LED MIMO VLC system with SSK scheme, where, the number of active LEDs is 1. The possible symbol combinations are $[1, 0, 0, 0]^T$, $[0, 1, 0, 0]^T$, $[0, 0, 1, 0]^T$, and $[0, 0, 0, 1]^T$, where, $[.]^T$ denotes the transpose operation. Both in SSK and GSSK, it is observed that, occurrence of any individual symbol or several patterns of the symbols continuously causes non-uniform illumination at individual LED level. Further, in SSK, the spectral efficiency (expressed in bits per channel use (bpcu)) is limited by the number of LEDs. In GSSK, it is limited by both the number of LEDs and active LEDs. Rest of the schemes mentioned earlier, i.e., SMP, SM, GSM, DCM, and QCM achieve any desired spectral efficiency for a given number of LEDs at the cost of bit error rate performance. However, uniformity in illumination at both system level and individual LED level has not been considered in these works. In [9], a coding scheme that provides uniform illumination at system level has been proposed. However, the scheme in [9] does not ensure uniform illumination at individual LED level. For a 2×2 MIMO VLC system, an optimal constellation design has been presented in [10] and spatial modulation schemes along with dimming control have been proposed in [11] and [12]. Nevertheless, uniform illumination at both system and individual LED levels has not been considered. Hence, in this paper we design codes that mitigate these non-uniform illumination issues.

The contributions of this work are as follows.

- We design codes that achieve uniform illumination at system level and also at individual LED level.
- We show the effect of transmit power and spectral efficiency on the bit error rate (BER) performance of the proposed codes for number of LEDs, N_t equal to 2, 3, and 4, with suitable expressions for spectral efficiency.
- We present the BER performance of the proposed codes with memory-based and memory less decoding along with bounds on the computational complexity involved in the decoding schemes.
- We also numerically analyze the impact of channel state information (CSI) on the BER performance by assuming perfect CSI is available only once in every fixed time interval, t_c, for different values of t_c. We use the same CSI for t_c time duration until the new CSI is available.

The remainder of this paper is organized as follows. In Section 2, we discuss the system model considered to implement the proposed codes. We present the proposed codes in Section 3. In Section 4, we analyze the numerical results for the proposed codes. Some concluding remarks and future scope are discussed in Section 5.

Notation: We use capital letters in bold and underline to denote matrices and capital letters with underline to denote vectors. We use $\lfloor . \rfloor$, $\mathbb{N}_0$, $[.]^T$, $\text{mod}(a, b)$, $||.||^2$, $|.|_c$, $|.|$, and $\mathbb{N}_0 \backslash \{.\}$ to denote floor operation, set of non-negative integers, transpose operation, a modulo b, Euclidean distance square, cardinality of any set, absolute value, and the set $\mathbb{N}_0$ excluding the elements in the set $\{.\}$, respectively. We use $\binom{a}{b}$ for $a!/((a-b)!b!)$, where, $a!$ denotes factorial of a.

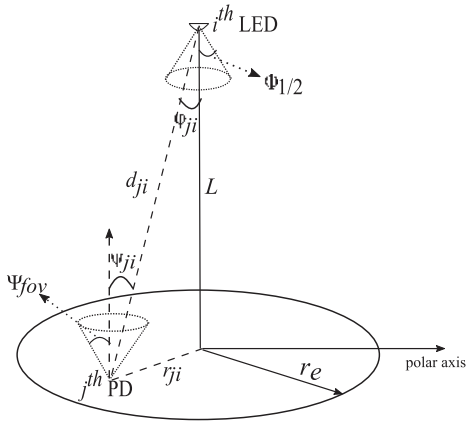

Fig. 2. Figure showing LED and PD parameters.

2. System Model

The system model considered to implement the proposed codes is shown in Fig. 1. At the transmitter (Tx), the input data is passed through the proposed encoder, where, the data is coded and modulated as per the desired brightness level (controlled by A) and desired spectral efficiency. The output of the proposed encoder are the symbols which are then transmitted through the LEDs. We consider an additive white Gaussian noise (AWGN) channel as in [13], [14] and with this consideration, the received symbol at the photo detector (PD), $\underline{\mathrm{Y}}$ is given as follows.

$$\underline{\mathrm{Y}} = \underline{\mathbf{H}}\,\underline{\mathrm{X}} + \underline{\mathrm{N}},$$

where, $\underline{\mathrm{X}}$ is the input symbol, $\underline{\mathrm{N}}$ is the AWGN noise, and $\underline{\mathbf{H}}$ is the channel gain matrix given by

$$\underline{\mathbf{H}} = \begin{bmatrix} h_{11} & h_{12} & h_{13} & \dots & h_{1\mathrm{N}_t} \\ h_{21} & h_{22} & h_{23} & \dots & h_{2\mathrm{N}_t} \\ \vdots & \vdots & \vdots & \ddots & \vdots \\ h_{\mathrm{N}_r 1} & h_{\mathrm{N}_r 2} & h_{\mathrm{N}_r 3} & \dots & h_{\mathrm{N}_r \mathrm{N}_t} \end{bmatrix},$$

where, h_{ji} is the direct current (DC) channel gain between j^{th} PD and i^{th} LED, N_r is the number of PDs, and N_t is the number of LEDs. At the receiver (Rx), the received symbols are decoded by the memory-based or memory less decoder, which are explained in detail in Section 3.

2.1 VLC Channel

The DC channel gain between the j^{th} PD and i^{th} LED [15], [16] is given as

$$h_{ji} = \begin{cases} \frac{(n+1)A_D R_p \cos(\phi_{ji})^n T(\psi_{ji}) g(\psi_{ji}) \cos(\psi_{ji})}{2\pi d_{ji}^2}, & \psi_{ji} \in [0,\ \psi_{fov}], \\ 0, & \psi_{ji} > \psi_{fov}, \end{cases}$$

where, n is the order of Lambertian radiation pattern given by $n = -1/\log_2(\cos(\Phi_{1/2}))$ such that $\Phi_{1/2}$ is the angle at half power of LED, A_D denotes the detection area of the PD at the Rx, R_p denotes the responsivity of the PD, $T(\psi_{ji})$ represents the gain of the optical filter used at the Rx, where, ψ_{ji} is the angle of incidence at the j^{th} PD from i^{th} LED as shown in Fig. 2, d_{ji} is the distance between the j^{th} PD and the i^{th} LED, $g(\psi_{ji})$ represents the gain of the optical concentrator, ψ_{fov} is the field of view of the PD at the Rx as shown in Fig. 2, and ϕ_{ji} angle of emission at the i^{th} LED with respect to j^{th} PD.

We consider uniform movement of the Rx in the receiver plane [17] and with this consideration, the final channel gain between the j^{th} PD and the i^{th} LED [17] is given by

$$h_{ji} = \frac{(n+1)CL^{n+1}}{\left(r_{ji}^2 + L^2\right)^{\frac{n+3}{2}}},$$

where, L is the vertical distance from the i^{th} LED to surface, r_{ji} is the radial distance between the j^{th} PD and i^{th} LED from top view as shown in Fig. 2, r_e is the LED coverage distance from the top view, and $C = \frac{1}{2\pi} A_D R_p T(\psi_{ji}) g(\psi_{ji})$. In the next section, the proposed codes along with the decoding mechanisms are discussed.

3. Proposed Codes

To maintain uniformity in illumination over time, the total transmit power by the system has to remain constant in each time slot. Let $\underline{\mathrm{X}} = [\mathrm{X}_1,\ \mathrm{X}_2, \ldots, \mathrm{X}_{\mathrm{N}_t}]^T$, where $[.]^T$ denotes transpose operation, be such that,

$$\sum_{i=1}^{\mathrm{N}_t} \mathrm{X}_i = \mathrm{A}, \tag{1}$$

where, A is the total transmit power per slot and X_i is the transmit power of the i^{th} LED, and hence, $\mathrm{X}_i \geq 0$. Codes have been designed in [9] satisfying (1). However, this constraint alone does not ensure uniformity in illumination at LED level. This is because, in real-time, the symbols can occur in any pattern and the codes designed in [9] does not ensure flicker mitigation at individual LED level. Human eyes cannot perceive light intensity changes if they occur within the maximum flickering time period (MFTP) which is 5 ms [18]. Next, we present an example highlighting the non-uniform illumination issue in [9].

Example: Consider the symbols from [9] given below, for $\mathrm{N}_t = 4$, $\mathrm{A} = 3$, and $\eta = 4$ *bpcu*, where, we can see (1) alone cannot ensure uniform illumination at individual LED level.

$[0,\ 0,\ 0,\ 3]^T$, $[0,\ 0,\ 3,\ 0]^T$, $[0,\ 3,\ 0,\ 0]^T$, $[3,\ 0,\ 0,\ 0]^T$, $[0,\ 1,\ 2,\ 0]^T$, $[1,\ 0,\ 0,\ 2]^T$,
$[0,\ 2,\ 1,\ 0]^T$, $[2,\ 0,\ 0,\ 1]^T$, $[1,\ 0,\ 2,\ 0]^T$, $[0,\ 1,\ 0,\ 2]^T$, $[1,\ 2,\ 0,\ 0]^T$, $[2,\ 0,\ 1,\ 0]^T$,
$[0,\ 0,\ 1,\ 2]^T$, $[0,\ 2,\ 0,\ 1]^T$, $[2,\ 1,\ 0,\ 0]^T$, $[0,\ 0,\ 2,\ 1]^T$.

It can be seen that if any specific symbol occur continuously, one or more LEDs will suffer from non-uniform illumination. For example, if the symbol $[0,\ 0,\ 0,\ 3]^T$ occurs continuously for more than 5 *ms*, then, flicker is perceived for the first three LEDs. This can also happen for several patterns of symbols transmitted. One such pattern where the fourth LED suffers from flicker is $[0,\ 0,\ 3,\ 0]^T$, $[0,\ 3,\ 0,\ 0]^T$, $[3,\ 0,\ 0,\ 0]^T$, and $[0,\ 1,\ 2,\ 0]^T$. Motivated by this, we consider the following two design constraints

- Constant power transmission in each time slot which provides uniform illumination across time,
- Uniform average illumination at individual LED level.

To achieve these, we propose memory-based codes, where, each message sequence is mapped to one or more symbols.

3.1 Design Overview

The symbol $\underline{\mathrm{X}}$ can be written as

$$\underline{\mathrm{X}} = \frac{\mathrm{A}}{\mathrm{M}} \left[\mathrm{m}_1,\ \mathrm{m}_2, \ldots, \mathrm{m}_{\mathrm{N}_t}\right]^T,\ \text{where,} \sum_{i=1}^{\mathrm{N}_t} \mathrm{m}_i = \mathrm{M}, \tag{2}$$

$\mathrm{m}_i \in \mathbb{N}_0$, such that $\mathbb{N}_0$ is the set of non-negative integers and $\mathrm{M} \in \mathbb{N}_0 \backslash \{0\}$. Since each entry of the symbol corresponds to the power of an LED, the value of m_i is greater than or equal to zero

for $1 \leq i \leq N_t$. We find the non-negative integer solutions to $\sum_{i=1}^{N_t} m_i = M$. Let these solutions be represented as a set $\mathcal{X}$. We then map one or more symbols from this set to each of the message sequences such that the design constraints are satisfied. The symbols are chosen based on the following guidelines:

1) To achieve uniform illumination, we first choose the symbols that have least difference between the transmit powers of active LEDs. Let this least difference be denoted by P_{diff}, then,
$$P_{\text{diff}} = \min_{\forall\, \underline{X} \in \mathcal{X}} \{\max\{X_i\} - \min\{X_i\}\}\,,\ i \in \{1, 2, \ldots, N_t\}\,\&\, X_i \neq 0.$$
2) In case the least difference is same, we consider the symbols with least average absolute difference in the transmit power of active LEDs. Let this least average absolute difference be denoted by P_{abs}. Let $\mathcal{X}'$ denote the set of symbols with equal P_{diff}, then,
$$P_{abs} = \min_{\forall\, \underline{X} \in \mathcal{X}'} \left\{ \frac{1}{\binom{N_a}{2}} \sum_{i=1}^{N_t - 1} \sum_{j=i+1}^{N_t} |X_i - X_j| \right\},\ i,\ j \in \{1, 2, \ldots, N_t\}\,\&\, X_i,\ X_j \neq 0\,,$$
where, N_a is the number of active LEDs.
3) In case both P_{diff} and P_{abs} are same, we then choose the symbol that gives higher average transmit power of active LEDs denoted by P_{avg}. This is because, the typical channel gains in VLC are low (order of 10^{-5}) [16], [19] and symbols with higher P_{avg} will result in improved performance. Let $\mathcal{X}''$ denotes the set of symbols with same P_{diff} and P_{abs}, then, the P_{avg} is given as follows
$$P_{avg} = \max_{\forall\, X \in \mathcal{X}''} \left\{ \frac{1}{N_a} \sum_{i=1}^{N_t} X_i \right\},\ i \in \{1, 2, \ldots, N_t\}\,\&\, X_i \neq 0.$$

For the proposed code, from (2), the value of A is used to control total transmit power per symbol so that desired brightness levels can be achieved and the value of M is varied to control the spectral efficiency which is elaborated in Section 3.5. Consider the following code designs for various values of N_t.

3.2 Code Design for $N_t = 2$

The symbol, $\underline{X} = [X_1,\ X_2]^T$ can be written as
$$\underline{X} = \frac{A}{M}\,[m_1,\ m_2]^T\,,\ \text{where,} \sum_{i=1}^{2} m_i = M.$$
The general form of the symbol for any given value of M is
$$\underline{X} = \frac{A}{M}\,[q,\ M - q]^T\,,$$
where, $q \in \mathbb{N}_0$ and $q \leq M$. Next, the symbols formed are mapped to message sequences as follows.
$$\underline{X} = \begin{cases} \frac{A}{2}\,[1,\ 1]^T\,, & \text{if} \quad X_i = M/2\ \forall\ i \in \{1, 2\}, \\ \frac{A}{M}\,[q,\ M - q]^T\ ,\ \frac{A}{M}\,[M - q,\ q]^T\,, & \text{otherwise.} \end{cases}$$

When $X_i = M/2\ \forall\ i \in \{1, 2\}$, both the LEDs are ON and each of them is transmitting the same power. Thus, even if the symbol $A/2[1,\ 1]^T$ is transmitted continuously, the two design constraints are satisfied. Hence, one of the message sequences mapped to such symbol will have only one symbol assigned. When $q \neq M/2$, the message sequences are mapped to two symbols and they are alternately transmitted when the same message sequence next appears. Each message sequence is assigned with symbol states denoted by $\mathbf{S}_f$ for $f \in \{0, 1, \ldots, k-1\}$, where k is the total number of symbols mapped. If k symbols are mapped to g^{th} message sequence, these

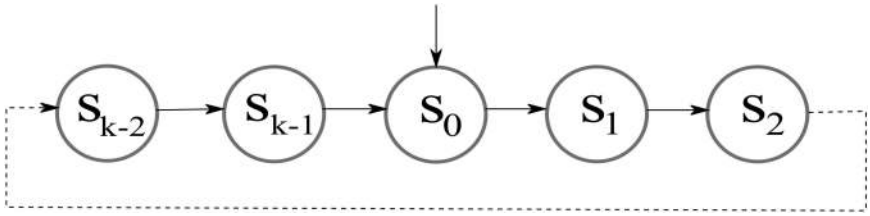

Fig. 3. Transmitted symbol states in a k states symbol mapping.

symbols mapped are given by $\underline{X}^g(\mathbf{S}_f)$ for $f \in \{0, 1, \ldots, k-1\}$. For example, if a message sequence is mapped to two symbols, then it has two symbols states denoted by $\mathbf{S}_0$ and $\mathbf{S}_1$ such that symbol in $\mathbf{S}_0$ is transmitted when the message sequence appears for the first time and symbol in $\mathbf{S}_1$ is transmitted when the same message sequence appears for the second time. On next appearance of the same message sequence, symbol in $\mathbf{S}_0$ is transmitted again and this process repeats as shown in Fig. 3. The value of k is 1 when $X_i = M/2 \ \forall \ i \in \{1, 2\}$ and 2 otherwise. Next, we present an example to illustrate this.

Example: Consider $M = 6$ and $N_t = 2$. Then, the symbol mapping for $\eta = 2$ bpcu is given as follows.

$\underline{X}^0(\mathbf{S}_0) = A/6[6, 0]$, $\underline{X}^0(\mathbf{S}_1) = A/6[0, 6]$ are mapped to [0 0],
$\underline{X}^1(\mathbf{S}_0) = A/6[3, 3]$ is mapped to [0 1],
$\underline{X}^2(\mathbf{S}_0) = A/6[2, 4]$, $\underline{X}^2(\mathbf{S}_1) = A/6[4, 2]$ are mapped to [1 0],
$\underline{X}^3(\mathbf{S}_0) = A/6[1, 5]$, $\underline{X}^3(\mathbf{S}_1) = A/6[5, 1]$ are mapped to [1 1].
Next, we illustrate the code design for $N_t = 3$.

3.3 Code Design for $N_t = 3$

The symbol, $\underline{X} = [X_1, \ X_2, \ X_3]^T$ can be written as

$$\underline{X} = \frac{A}{M}[m_1, \ m_2, \ m_3]^T, \ \text{where}, \sum_{i=1}^{3} m_i = M.$$

The general form of the symbol for any given value of M is

$$\underline{X} = \frac{A}{M}[q, \ r, \ M - q - r]^T,$$

where, $q, \ r \in \mathbb{N}_0$ and $q + r \leq M$. Next, we illustrate the code design for $N_t = 4$.

3.4 Code Design for $N_t = 4$

The symbol $\underline{X} = [X_1, \ X_2, \ X_3, \ X_4]^T$ can be written as

$$\underline{X} = \frac{A}{M}[m_1, \ m_2, \ m_3, \ m_4]^T, \ \text{where}, \sum_{i=1}^{4} m_i = M.$$

Whenever $N_a = 1$, any three among $m_1, \ m_2, \ m_3, \ m_4$ has to be zero and $\underline{X}$ will have four states with the symbols, $[A, \ 0, \ 0, \ 0]^T$, $[0, \ A, \ 0, \ 0]^T$, $[0, \ 0, \ A, \ 0]^T$, and $[0, \ 0, \ 0, \ A]^T$. Hence, when $N_a = 1$, all the symbols generated can be mapped to only one message sequence to satisfy the design constraints. When $N_a = 2$, any two of $m_1, \ m_2, \ m_3, \ m_4$ has to be zero and one possible symbol $\underline{X}$ for such case is given as $A/M[0, \ q, \ M - q, \ 0]^T$, $q < M$ and $q \in \mathbb{N}_0 \backslash \{0\}$. The possible combinations if $q = M - q$ are $A/M[0, \ q, \ M - q, \ 0]^T$, $A/M[q, \ 0, \ 0, \ M - q]^T$, $A/M[q, \ 0, \ M - q, \ 0]^T$, $A/M[0, \ q, \ 0, \ M - q]^T$, $A/M[0, \ 0, \ q, \ M - q]^T$, and $A/M[q, \ M - q, \ 0, \ 0]^T$, where, each consecutive pairs form mappings with two symbol states so that total three distinct mappings are formed.

TABLE 1
Symbols Mapping to Message Sequences for $N_t = 4$, $M = 4$, and $\eta = 3$ bpcu

Symbol/Symbols	Message sequence:: Number of states
$\underline{X}^0(\mathbf{S}_0) = \frac{A}{4}[4,\ 0,\ 0,\ 0]^T$, $\underline{X}^0(\mathbf{S}_1) = \frac{A}{4}[0,\ 4,\ 0,\ 0]^T$, $\underline{X}^0(\mathbf{S}_2) = \frac{A}{4}[0,\ 0,\ 4,\ 0]^T$, $\underline{X}^0(\mathbf{S}_3) = \frac{A}{4}[0,\ 0,\ 0,\ 4]^T$	[0 0 0]::4
$\underline{X}^1(\mathbf{S}_0) = \frac{A}{4}[2,\ 0,\ 0,\ 2]^T$, $\underline{X}^1(\mathbf{S}_1) = \frac{A}{4}[0,\ 2,\ 2,\ 0]^T$	[0 0 1]::2
$\underline{X}^2(\mathbf{S}_0) = \frac{A}{4}[2,\ 2,\ 0,\ 0]^T$, $\underline{X}^2(\mathbf{S}_1) = \frac{A}{4}[0,\ 0,\ 2,\ 2]^T$	[0 1 0]::2
$\underline{X}^3(\mathbf{S}_0) = \frac{A}{4}[2,\ 0,\ 2,\ 0]^T$, $\underline{X}^3(\mathbf{S}_1) = \frac{A}{4}[0,\ 2,\ 0,\ 2]^T$	[0 1 1]::2
$\underline{X}^4(\mathbf{S}_0) = \frac{A}{4}[1,\ 1,\ 1,\ 1]^T$	[1 0 0]::1
$\underline{X}^5(\mathbf{S}_0) = \frac{A}{4}[1,\ 2,\ 0,\ 1]^T$, $\underline{X}^5(\mathbf{S}_1) = \frac{A}{4}[2,\ 1,\ 1,\ 0]^T$, $\underline{X}^5(\mathbf{S}_2) = \frac{A}{4}[1,\ 0,\ 2,\ 1]^T$, $\underline{X}^5(\mathbf{S}_3) = \frac{A}{4}[0,\ 1,\ 1,\ 2]^T$	[1 0 1]::4
$\underline{X}^6(\mathbf{S}_0) = \frac{A}{4}[1,\ 1,\ 0,\ 2]^T$, $\underline{X}^6(\mathbf{S}_1) = \frac{A}{4}[1,\ 1,\ 2,\ 0]^T$, $\underline{X}^6(\mathbf{S}_2) = \frac{A}{4}[0,\ 2,\ 1,\ 1]^T$, $\underline{X}^6(\mathbf{S}_3) = \frac{A}{4}[2,\ 0,\ 1,\ 1]^T$	[1 1 0]::4
$\underline{X}^7(\mathbf{S}_0) = \frac{A}{4}[2,\ 1,\ 0,\ 1]^T$, $\underline{X}^7(\mathbf{S}_1) = \frac{A}{4}[1,\ 0,\ 1,\ 2]^T$, $\underline{X}^7(\mathbf{S}_2) = \frac{A}{4}[1,\ 2,\ 1,\ 0]^T$, $\underline{X}^7(\mathbf{S}_3) = \frac{A}{4}[0,\ 1,\ 2,\ 1]^T$	[1 1 1]::4

Similarly, if $q \neq M - q$, three mappings can be formed, but each with four symbol states. When $N_a = 3$, any one among m_1, m_2, m_3, m_4 has to be zero and mappings are formed with four states. Similar possible mappings can be formed for $N_a = 4$.

From the above code design details, the two design constraints can be rewritten as follows.

- Constant power transmission in each time slot to provide uniform illumination across time is achieved by $\sum_{i=1}^{N_t} X_i = A$ which is (1).
- Uniform average illumination, i.e., uniformity in illumination on an average over time at individual LED level which is achieved by the following constraint

$$\{X_1\} = \{X_2\} = \cdots = \{X_{N_t}\}, \tag{3}$$

where, $\{X_i\}$ denotes the set of transmitted power values by the i^{th} LED considering all the symbols mapped to any message sequence. Next, we present an example to illustrate that both these design constraints are satisfied by the proposed code.

Example: Consider the last row of Table 1. For all the symbols mapped to $\underline{X}^7$, $\sum_{i=1}^{N_t} X_i = A$. Hence, the first constraint, i.e., (1) is satisfied. Similarly, from $\{X_1\} = \{2, 1, 1, 0\}$, $\{X_2\} = \{1, 0, 2, 1\}$, $\{X_3\} = \{0, 1, 1, 2\}$, and $\{X_4\} = \{1, 2, 0, 1\}$, it is observed that the set of transmitted power values are same for all the four LEDs, which satisfy (3). Hence, the second design constraint is also satisfied. Although we have illustrated the codes for $N_t = 2, 3$, and 4. Based on (1), (2), (3), and the guidelines mentioned earlier in this section, the proposed code design can be generalized to any larger value of N_t. The mappings for $N_t = 4$, $M = 4$, and $\eta = 3$ bpcu are given in Table 1. It is observed that A can be varied to achieve the desired brightness level. However, the variation of spectral efficiency with M needs to be analyzed and is presented next.

3.5 Expression for Spectral Efficiency

3.5.1 Spectral Efficiency for Odd N_t: The number of symbol states for a possible mapping denoted by k is given as

$$k = \begin{cases} 1, & \text{if } X_i = M/N_t \in \mathbb{N}_0 \ \forall\ i \in \{1, 2, \ldots, N_t\}, \\ N_t, & \text{otherwise.} \end{cases} \tag{4}$$

Consider the following example, where, the calculation of k is explained.

Example: Let $N_t = 3$, $M = 3$, and $N_a \leq N_t$, then the possible combinations are A/3[1, 1, 1], A/3[3, 0, 0], A/3[0, 3, 0], A/3[0, 0, 3], A/3[1, 2, 0], A/3[0, 1, 2], A/3[2, 0, 1], A/3[2, 1, 0], A/3[0, 2, 1], and A/3[1, 0, 2]. From the design constraints, mapping is done as follows. The symbols A/3[3, 0, 0], A/3[0, 3, 0], and A/3[0, 0, 3] are mapped to [0 0]. The symbol A/3[1, 1, 1]

is mapped to [0 1]. The symbols A/3[1, 2, 0], A/3[0, 1, 2], and A/3[2, 0, 1] are mapped to [1 0] and the symbols A/3[2, 1, 0], A/3[0, 2, 1], and A/3[1, 0, 2] are mapped to [1 1]. It can be seen that, for the first, third, and fourth mappings when $N_a < N_t$, k is equal to N_t. For the second mapping, when $N_a = N_t$ and $X_i = 1\ \forall\ i \in \{1, 2, 3\}$, the value of k is 1.

Using k, η is the largest integer that satisfies the following inequality

$$2^{\eta} \leq \frac{1}{N_t}\left\{\sum_{N_a=1}^{\min(N_t-1,\,M)} \binom{M-1}{N_a-1}\binom{N_t}{N_a} + \delta\right\} + \sigma, \tag{5}$$

where, δ and σ are defined for $M \geq N_t$ as follows

$$\delta = \begin{cases} \binom{M-1}{N_t-1}, & \text{if } \mod(M,\ N_t) \neq 0, \\ \binom{M-1}{N_t-1} - 1, & \text{if } \mod(M,\ N_t) = 0, \end{cases}$$

and

$$\sigma = \begin{cases} 1, & \text{if } \mod(M,\ N_t) = 0, \\ 0, & \text{if } \mod(M,\ N_t) \neq 0. \end{cases}$$

In (5), $\sum_{N_a=1}^{\min(N_t-1,\,M)} \binom{M-1}{N_a-1}\binom{N_t}{N_a}$ represents the total number of combinations for $1 \leq N_a \leq N_t - 1$ and this is multiplied by $1/N_t$, since each mapping requires N_t symbols for $1 \leq N_a \leq N_t - 1$. The term σ accounts for the mappings that are possible when $N_a = N_t$. Hence, the final expression for η is calculated as

$$\eta = \left\lfloor \log_2\left(\frac{1}{N_t}\left\{\sum_{N_a=1}^{\min(N_t-1,\,M)} \binom{M-1}{N_a-1}\binom{N_t}{N_a} + \delta\right\} + \sigma\right)\right\rfloor. \tag{6}$$

3.5.2 Spectral Efficiency for Even N_t*:* Unlike the possibility of only two different values of k when N_t is odd, several values for the k is possible when N_t is even and it depends on the values of M and N_a. Here, value of k is given by the following expression

$$k = \frac{N_t}{\text{HCF}}(Q), \tag{7}$$

where, HCF(Q) denotes the highest common factor (HCF) of the elements in the set, $Q = \{Q_u\}$. Here, Q_u denotes the number of times a transmit power value has occurred in the $\underline{X}$ and $\forall\ u \in \{1, 2, \ldots,$ number of distinct transmit power values in $\underline{X}\}$. The expression in (7) can be proved as follows.

Let any symbol, $\underline{X} = [X_1,\ X_2,\ \ldots,\ X_{N_t}]^T$, $\min\{Q\} = 1$, and $\exists\ Q_u > 1$. Now, let that unique transmit power value in $\underline{X}$ be X_i. Then, to satisfy the design constraints, this X_i has to transmitted by all the N_t LEDs, and hence, $k = N_t$. Next, let each Q_u be a multiple of 2 and $\min\{Q\} = 2$. Then, the design constraints are satisfied with $k = N_t/2$. Similarly, let each Q_u be a multiple of U and $\min\{Q\} = U$, which implies that U is the HCF(Q). Then, with $k = N_t/U = N_t/\text{HCF(Q)}$, the design constraints are satisfied. For example, consider the symbol in first row of Table 1, $A/4[4,\ 0,\ 0,\ 0]^T$. For this symbol, $Q_1 = 1$ (number of 4 s are 1) and $Q_2 = 3$ (number of 0 s are 3). From (7), $k = 4$ since, HCF($\{1, 3\}$) is 1. Hence, the four symbols in first row of Table 1. In (7), N_t is divided by HCF(Q) to get the number of symbol states that satisfy the second design constraint, i.e., (3). Consider the following example that illustrates (3) and (7).

Example:

1) Let $N_t = 6$, $N_a = 6$, $M = 12$, and a symbol, A/12[1, 3, 2, 3, 1, 2]. Given this, using (7), $Q = 2$ and hence, $k = 3$. The given symbol along with the other two symbols A/12[3, 1, 1, 2, 2, 3] and A/12[2, 2, 3, 1, 3, 1] forms the 3 symbol states for a message sequence mapping.

Algorithm 1: Algorithm for Memory-Based Decoding.

1: **for** $g = 0$ to $2^{\eta} - 1$ **do**
2: $\mathbf{S}(g) \leftarrow 0$
3: **end for**
4: $\hat{\underline{X}} = \arg\min||\underline{Y} - \underline{\mathbf{H}}\,\underline{X}^{g}(\mathbf{S}(g))||^2$ for $g \in \{0, 1, \ldots, 2^{\eta} - 1\}$
5: If g^{th} message sequence is decoded, then $\mathbf{S}(g) \leftarrow \mathbf{S}(g) + 1$
6: **if** $\mathbf{S}(g) == \mathbf{S}_{\max}(g) + 1$ **then**
7: $\mathbf{S}(g) \leftarrow 0$
8: **end if**
9: Repeat from 4

2) Let $N_t = 8$, $N_a = 4$, $M = 6$, and a symbol, A/6[1, 1, 2, 2, 0, 0, 0, 0]. Given this, using (7), $Q = 2$ and hence, $k = 4$. The other three symbols that can be grouped with the given symbol are A/6[0, 0, 1, 1, 2, 2, 0, 0], A/6[0, 0, 0, 0, 1, 1, 2, 2], and A/6[2, 2, 0, 0, 0, 0, 1, 1].

Considering the exact number of states when $Q = 1$, $\mathrm{mod}(N_t, N_a) = 1$, $X_i \in \{\frac{M}{N_a}, 0\}$, and N_t number of states in all other cases, the lower bound on the value of η when N_t is even is given as follows

$$\eta \geq \left\lfloor \log_2 \left(\sum_{N_a=1}^{\min(N_t, M)} \left\{ \frac{1}{N_t} \left(\binom{M-1}{N_a - 1} \binom{N_t}{N_a} - \Lambda_1 \right) + \Lambda_2 \right\} \right) \right\rfloor, \tag{8}$$

where,

$$\Lambda_1 = \begin{cases} \binom{N_t}{N_a}, & \text{if mod}\,(N_t, N_a) = 0 \text{ and } X_i \in \left\{\frac{M}{N_a}, 0\right\}, \\ 0, & \text{otherwise,} \end{cases}$$

and

$$\Lambda_2 = \begin{cases} \frac{N_a}{N_t} \binom{N_t}{N_a}, & \text{if mod}\,(N_t, N_a) = 0 \text{ and } X_i \in \left\{\frac{M}{N_a}, 0\right\}, \\ 0, & \text{otherwise.} \end{cases}$$

Since $\Lambda_2 = \frac{N_a}{N_t}\Lambda_1$, (8) can be rewritten as

$$\eta \geq \left\lfloor \log_2 \left(\sum_{N_a=1}^{\min(N_t, M)} \left\{ \frac{1}{N_t} \left(\binom{M-1}{N_a - 1} \binom{N_t}{N_a} - \Lambda_1 \right) + \frac{N_a}{N_t}\Lambda_1 \right\} \right) \right\rfloor.$$

Next, we present the decoding mechanisms for the proposed codes.

3.6 Decoding of Proposed Codes

3.6.1 Memory Less Decoding: In memory less decoding, we compute the Euclidean distance of the received symbol from each one of the symbols. The detection rule is given as

$$\hat{\underline{X}} = \arg\min_{\forall \underline{X}} ||\underline{Y} - \underline{\mathbf{H}}\,\underline{X}||^2.$$

3.6.2 Memory-Based Decoding: The decoding of the proposed codes by memory-based decoding is presented in Algorithm 1. Here, we compute Euclidean distance only over 2^{η} symbols, based on the knowledge that for any message sequence, symbol in 1^{st} state is transmitted first. In Algorithm 1, $\mathbf{S}_{\max}(g)$ denotes maximum symbol state of the g^{th} message sequence, $\mathbf{S}(g)$ denotes current symbol state of the g^{th} message sequence, and $\underline{X}^{g}(\mathbf{S}(g))$ denotes symbol at $\mathbf{S}(g)$ mapped to the g^{th} message sequence. Next, we discuss the computational complexity of the proposed codes.

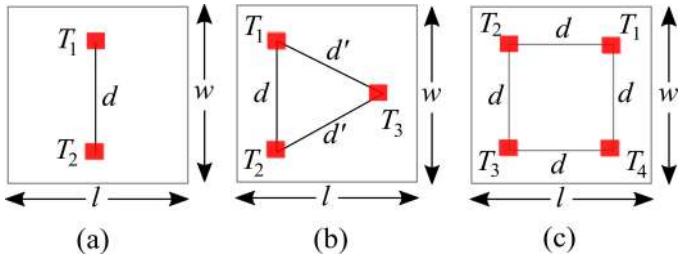

Fig. 4. Figure showing LED positions for (a). $N_t = 2$, (b). $N_t = 3$, and (c). $N_t = 4$.

3.7 Computational Complexity

For memory-based decoding, the computations are independent of the number of symbol states associated with each message sequence and depends only on the number of message sequences. Hence, the number of computations required for memory-based decoding is 2^{η}. For memory less decoding, we define upper and lower bounds on the number of computations as follows. When N_t is odd, the number of symbol states for a message sequence is given by (5). Let the number of computations be Ω whose range is equal to

$$N_t(2^{\eta} - 1) + 1 \leq \Omega \leq N_t\, 2^{\eta}.$$

When N_t is even, the range of Euclidean distance computations is given as follows

$$2^{\eta} < \Omega \leq N_t 2^{\eta}.$$

In the next section, we present the numerical results for the proposed codes.

4. Numerical Results

To compute the numerical results, we consider the receiver moving uniformly in different directions in the receiver plane with constant speed. The current location of the receiver is determined based on the previous location. Let the previous location of the receiver be (x_b, y_b), where, $x_b = r_b \cos\theta_b$ and $y_b = r_b \sin\theta_b$. Then, the current location (x_{b+1}, y_{b+1}) is given by $x_{b+1} = x_b + r_{b+1}\cos\theta_{b+1} = r_b\cos\theta_b + r_{b+1}\cos\theta_{b+1}$ and $y_{b+1} = y_b + r_{b+1}\sin\theta_{b+1} = r_b\sin\theta_b + r_{b+1}\sin\theta_{b+1}$. We assume that receiver plane is horizontal to the surface and generate θ_b uniformly from $[0, 2\pi)$. The position of LEDs from the top view is shown in Fig. 4(a), Fig. 4(b), and Fig. 4(c) for N_t equal to 2, 3, and 4, respectively. We assume the center of the room from top view as the reference point (0, 0). With this assumption, the position of T_1 and T_2 for $N_t = 2$ is (0, 1) and $(0, -1)$, respectively, and for $N_t = 3$, the position of T_1, T_2, and T_3 is $(-1, 1)$, $(-1, -1)$, and (1, 0), respectively. Similarly, for $N_t = 4$, the position of T_1, T_2, T_3, and T_4 is (1,1), $(-1, 1)$, $(-1, -1)$, and $(1, -1)$, respectively. To generate simulation results, we assume N_r equal to 1 for any value of N_t. However, note that the proposed codes can be implemented for any value of N_r.

Assuming all LEDs are identical and PDs are identical, the common parameters for simulation for any N_t and N_r, considered in this work are given in Table 2. In Fig. 5(a), the BER performance of the proposed codes for $N_t = 4$, $N_r = 1$, $\eta = 3$ bpcu, $M = 4$, $A = 4$, receiver speed $= 0.5$ m/sec, and symbol rate $= 10^7$ symbols/sec (3×10^7 bits/sec) is shown with memory less decoding, assuming perfect CSI is available at the Rx after every t_c time for t_c equal to 0.1 μs, 0.01 ms, 1 ms, 10 ms, and 20 ms. For t_c equal to 0.1 μs, BER continuously decreases with decrease in the considered noise power, since CSI is available for every symbol for the considered symbol rate. For other values of t_c, it is observed that BER saturates faster with the higher values of t_c. The impact of t_c on the average number of correctly received information bits which is computed using (1-BER)η bpcu is shown in Fig. 5(b). It is observed that as $1/\sigma^2(dB)$ increases, (1-BER)η saturates to lower values with increase in t_c.

In Fig. 6(a) and Fig. 6(b), BER plots by varying A, for receiver speed $= 0.5$ m/sec, symbol rate $= 10^7$ symbols/sec, $N_r = 1$, $M = 4$, and $\eta = 3$ bpcu with memory less decoding are plotted for $N_t = 4$ and 3, respectively. It is seen that BER decreases as A increases, for the same channel conditions.

TABLE 2
Parameters for Simulation [17]

Parameter	Value
Vertical distance from LEDs to surface of PD, L	2.15 m
LED semi angle, $\Phi_{1/2}$	60°
PD FOV, ψ_{fov}	60°
PD responsivity, R_p	0.4 A/W
PD detection area, A_D	10^{-4} m^2
Optical filter gain, T	1
Length of the room, l	4 m
Width of the room, w	4 m
Distance between LEDs shown in Fig. 4, d	2 m
Receiver speed	0.5 m/sec
Symbol rate	10^7 $symbols/sec$

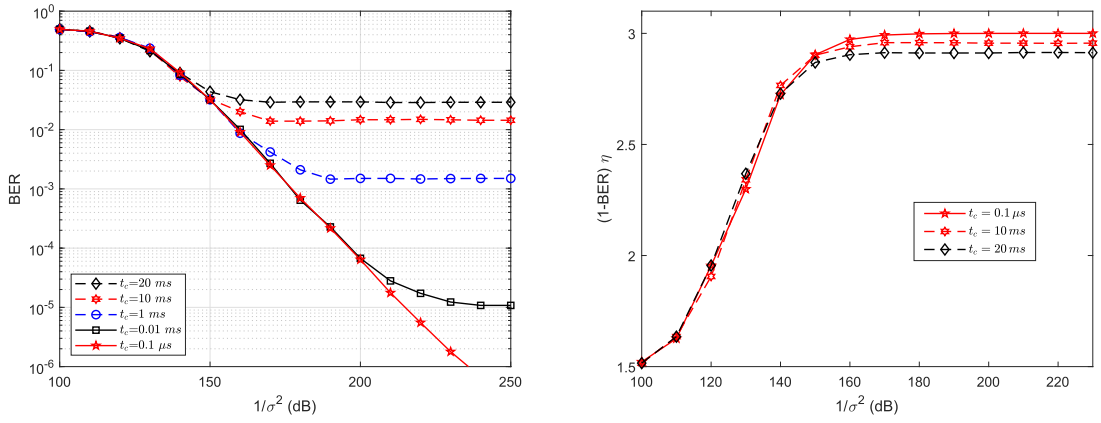

Fig. 5. (a). BER plots with memory less decoding, where, perfect CSI is available only at the receiver, once in every t_c time, for receiver speed = 0.5 m/sec, symbol rate = 10^7 symbols/sec, $N_t = 4$, $N_r = 1$, $\eta = 3$ bpcu, M = 4, and A = 4. (b). Figure showing impact of t_c on the number of correctly received information bits per channel use, for receiver speed = 0.5 m/sec, symbol rate = 10^7 symbols/sec, $N_t = 4$, $N_r = 1$, $\eta = 3$ bpcu, M = 4, and A = 4.

In Fig. 7(a), the BER performance of the memory less decoding is compared with memory-based decoding, where, symbols states at Tx and Rx are reset after every r_s symbol transmissions for receiver speed = 0.5 m/sec, symbol rate = 10^7 symbols/sec, $N_t = 4$, $N_r = 1$, $\eta = 3$ bpcu, M = 4, and A = 4. With these considerations, in Fig. 7(a), when $r_s = 1$, only the symbol in first state is transmitted for each of the message sequences. In this case, the decoding is performed on fewer symbols (2^η) when compared to memory less decoding, and hence, the BER performance of memory-based decoding for this value of r_s is better than that of memory less decoding. However, uniform illumination at individual LED level cannot be achieved for this value of r_s. The BER performance of memory-based decoding for $r_s = 10^6$ is also shown in Fig. 7(a). For this case, since the value of r_s is high, the illumination constraints are achieved. It is also observed that the BER performance decreases as r_s increases, since with increase in r_s, the duration of error propagation increases.

In Fig. 7(b), the BER performance of the proposed design with memory less decoding is compared with the state-of-the-art designs in [6] and [9] for A = 4, receiver speed = 0.5 m/sec,

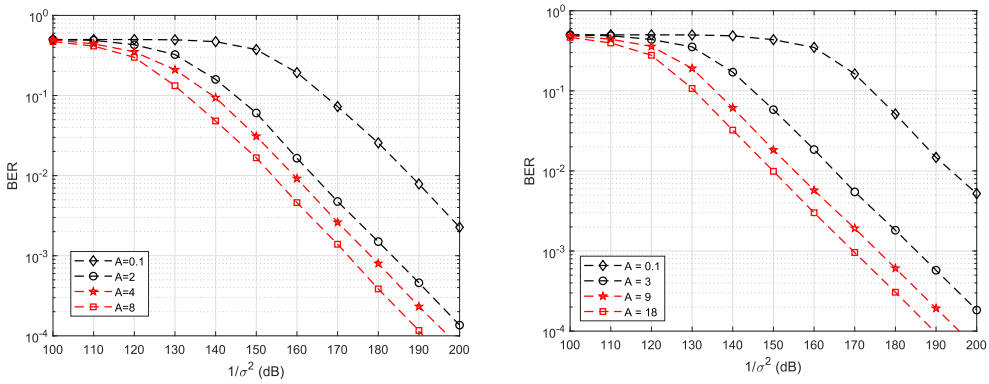

Fig. 6. BER plots by varying transmit power, A, for receiver speed = 0.5 m/sec, symbol rate = 10^7 symbols/sec with memory less decoding for (a). $N_t = 4$, $N_r = 1$, M = 4, and $\eta = 3$ bpcu. (b). $N_t = 3$, $N_r = 1$, M = 4, and $\eta = 3$ bpcu.

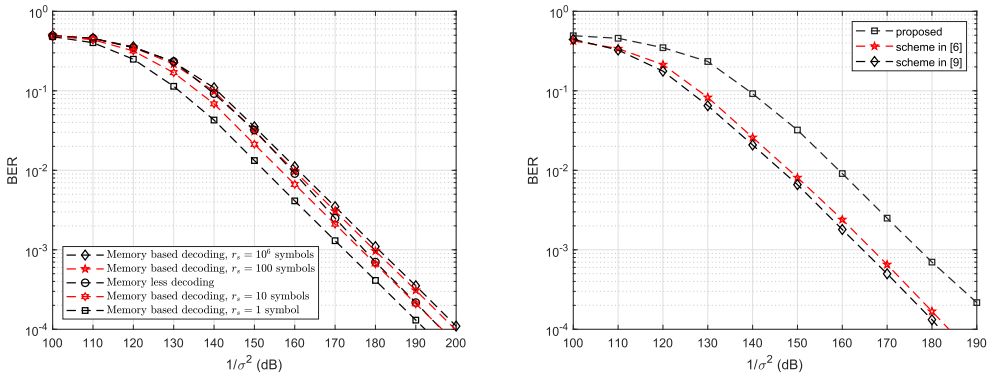

Fig. 7. (a) BER plots comparing memory less decoding and memory-based decoding, where, states are reset after every r_s symbol transmissions, for receiver speed = 0.5 m/sec, symbol rate = 10^7 symbols/sec, $N_t = 4$, $N_r = 1$, $\eta = 3$ bpcu, M = 4, and A = 4. (b) BER plots comparing the proposed design (with memory less decoding) for M = 4 with the design in [6] for $N_a = 2$ and [9] for $N_a \leq 2$ for A = 4, receiver speed = 0.5 m/sec, symbol rate = 10^7 symbols/sec, $N_t = 4$, $N_r = 1$, and $\eta = 3$ bpcu.

symbol rate = 10^7 symbols/sec, $N_t = 4$, $N_r = 1$, and $\eta = 3$ bpcu. It is seen that the proposed design performance is relatively poor compared to the existing designs since for the proposed design, the decoding is performed over more symbols as many of the message sequences are mapped to more than one symbol. However, the proposed design achieves uniform illumination at individual LED level which is not achieved by the existing designs. Further, the proposed design performance can be tuned using appropriate value of M and A.

In Fig. 8, the BER performance of the proposed design by varying η for A = 4, receiver speed = 0.5 m/sec, symbol rate = 10^7 symbols/sec, $N_t = 2$, and $N_r = 1$ with memory less decoding is plotted. It is observed that as η increases, the BER performance decreases.

In Table 3, we have compared the performance of the proposed design, code in [6], and the code in [9] in terms of variance in the total power transmitted by different LEDs for $N_t = 4$ for every Ξ symbol transmissions using the following expressions

$$\mu_e^{\Xi} = \frac{1}{N_t} \sum_{i=1}^{N_t} A_{T_{i,e}}^{\Xi},$$

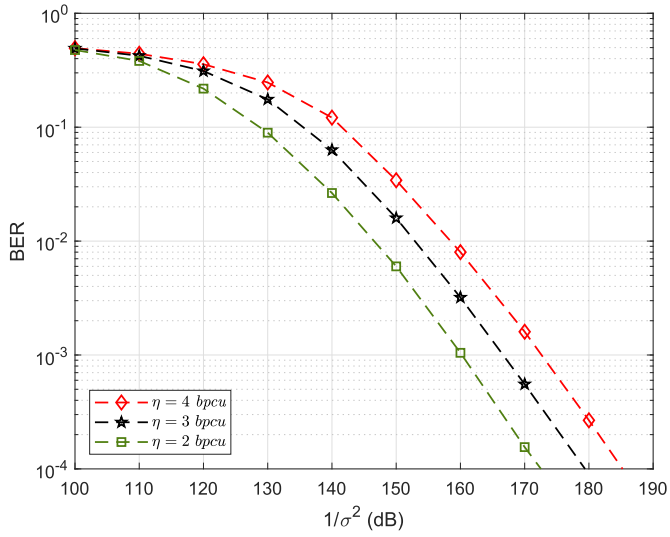

Fig. 8. BER plots comparing the proposed design by varying η, for A $= 4$, receiver speed $= 0.5$ m/sec, symbol rate $= 10^7$ symbols/sec, $N_t = 2$, and $N_r = 1$ with memory less decoding.

TABLE 3

Comparing the Proposed Design, Code in [6], and the Code in [9] in Terms of Variance in the Total Power Transmitted by Different LEDs for $N_t = 4$ for Every Ξ Symbol Transmissions for $\beta = 5000$ at 3 *bits/symbol*

Ξ	proposed design	code in [6]	code in [9]
50	5.129	56.828	99.480
100	5.281	117.83	198.51
500	5.285	576.79	1022.4
1000	5.171	1197.3	2021.2
10000	5.296	11648	19478

and

$$\sigma_{\Xi}^2 = \frac{1}{\beta N_t} \sum_{e=1}^{\beta} \sum_{i=1}^{N_t} \left(A_{T_{i,e}}^{\Xi} - \mu_e^{\Xi} \right)^2,$$

where, μ_e^{Ξ} is the mean of the power transmitted by the N_t LEDs in e^{th} iteration, $A_{T_{i,e}}^{\Xi}$ is total power transmitted by i^{th} LED in e^{th} iteration, and σ_{Ξ}^2 is the variance in the power transmitted by N_t LEDs for Ξ symbol transmissions for β iterations. For fair comparison of variance, the symbols of the compared codes were properly scaled such that the average power transmitted per symbol remains same. The variance is averaged for $\beta = 5000$ iterations at 3 *bits/symbol*. It is observed that the variance in the total power transmitted by different LEDs is significantly less for the proposed codes as compared to the codes in [6] and [9], and hence, the proposed design achieves uniformity in illumination so that the user perceives same illumination from different individual LEDs. Similarly, in Table 4, we have compared the proposed design, code in [6], and the code in [9] in terms of variance in the total power transmitted by individual LEDs for $N_t = 4$ for every Ξ symbol transmissions using the following equations

$$\mu_{T_{i,\beta}}^{\Xi} = \frac{1}{\beta} \sum_{e=1}^{\beta} A_{T_{i,e}}^{\Xi},$$

TABLE 4
Comparing the Proposed Design, Code in [6], and the Code in [9] in Terms of Variance in the Total Power Transmitted by Individual LEDs for $N_t = 4$ After every Ξ Symbol Transmissions for $\beta = 5000$ at 3 *bits/symbol*

Ξ	proposed design				code in [6]				code in [9]			
	T_1	T_2	T_3	T_4	T_1	T_2	T_3	T_4	T_1	T_2	T_3	T_4
50	5.329	5.065	5.42	4.956	62.88	62.22	62.04	61.77	97.849	102.45	101.07	96.14
100	5.373	5.147	5.021	5.468	123.82	127.42	124.80	124.44	202.91	206.94	198.05	199.54
500	5.227	5.100	5.232	5.369	610.96	625.22	614.77	618.60	996.91	994.63	1029.10	1002.6
1000	5.150	5.317	5.310	5.258	1184.6	1200.1	1186.1	1183.5	2006.9	2023	1979.3	1972.9
10000	5.219	5.479	5.275	5.195	12179	12423	12362	12185	20279	19343	19118	19152

and

$$\sigma^2_{T_{i,\beta}} = \frac{1}{\beta}\sum_{e=1}^{\beta}\left(\mathrm{A}^{\Xi}_{T_{i,e}} - \mu^{\Xi}_{T_{i,\beta}}\right)^2,$$

where, $\mu^{\Xi}_{T_{i,\beta}}$ is the mean of the total power transmitted by i^{th} LED in β iterations and for Ξ symbol transmissions, $\mathrm{A}^{\Xi}_{T_{i,e}}$ is the total power transmitted by i^{th} LED in e^{th} iteration for Ξ symbol transmissions, and $\sigma^2_{T_{i,\beta}}$ is the variance in the total power transmitted by the i^{th} LED in β iterations. It is observed that the variance in power transmitted by individual LEDs over time is significantly less for the proposed codes which ensures uniformity in illumination across time slots as compared to the state-of-the-art code designs for MIMO VLC. In the next section, we present some concluding remarks.

5. Conclusion

We have proposed memory-based codes under the constraints of constant total transmit power per symbol and same average transmit power per LED, where, these constraints helps to achieve uniformity in the illumination per LED and overall system across different time slots. We have shown the performance of the proposed codes in terms of various metrics like BER, consistency in illumination, and spectral efficiency with suitable expressions. We have also shown the impact of CSI on BER performance by assuming perfect CSI is available at the receiver only once in every fixed time interval, t_c and for different values of t_c. Compared to the existing state-of-the-art MIMO VLC codes, the proposed code design provides uniformity in illumination at the cost of reduced BER performance.The extension of the proposed scheme for multi-user MIMO VLC will be explored in future. In this direction, a multiple access control (MAC) protocol would be developed that exploits the dynamic link quality between fixed MIMO VLC transmitters and multiple moving VLC users. For a multi-user system, signal-to-interference-plus-noise ratio (SINR) based analysis will also be considered in future.

References

[1] D. Karunatilaka, F. Zafar, V. Kalavally, and R. Parthiban, "LED based indoor visible light communications: State of the Art," *IEEE Commun. Surv. Tut.*, vol. 17, no. 3, pp. 1649–1678, Jul.–Sep. 2015.
[2] Y. Gong, L. Ding, Y. He, H. Zhu, and Y. Wang, "Analysis of space shift keying modulation applied to visible light communications," in *Proc. IET Int. Conf. Inf. Commun. Technol.*, 2013, pp. 503–507.
[3] W. O. Popoola, E. Poves, and H. Haas, "Error performance of generalised space shift keying for indoor visible light communications," *IEEE Trans. Commun.*, vol. 61, no. 5, pp. 1968–1976, May 2013.
[4] T. Fath and H. Haas, "Performance comparison of MIMO techniques for optical wireless communications in indoor environments," *IEEE Trans. Commun.*, vol. 61, no. 2, pp. 733–742, Feb. 2013.
[5] R. Mesleh, R. Mehmood, H. Elgala, and H. Haas, "Indoor MIMO optical wireless communication using spatial modulation," in *Proc. IEEE Int. Conf. Commun.*, 2010, pp. 1–5.

[6] S. P. Alaka, T. L. Narasimhan, and A. Chockalingam, "Generalized spatial modulation in indoor wireless visible light communication," in *Proc. IEEE Global Commun. Conf.*, 2015, pp. 1–7.
[7] A. K. Gupta and A. Chockalingam, "Performance of MIMO modulation schemes with imaging receivers in visible light communication," *J. Lightw. Technol.*, vol. 36, no. 10, pp. 1912–1927, May 2018.
[8] R. Tejaswi, T. L. Narasimhan, and A. Chockalingam, "Quad-LED complex modulation (QCM) for visible light wireless communication," in *Proc. IEEE Wireless Commun. Netw. Conf.*, 2016, pp. 1–6.
[9] T. Uday, A. Kumar, and L. Natarajan, "Low PAPR coding scheme for uniform illumination in MIMO VLC," in *Proc. IEEE Globecom Workshops*, Abu Dhabi, UAE, 2018, pp. 1–6.
[10] H. B. Cai, J. Zhang, Y. J. Zhu, J. K. Zhang, and X. Yang, "Optimal constellation design for indoor 2 $\times$ 2 MIMO visible light communications," *IEEE Commun. Lett.*, vol. 20, no. 2, pp. 264–267, Feb. 2016.
[11] Y. Yang, Z. Zeng, J. Cheng, and C. Guo, "Spatial dimming scheme for optical OFDM based visible light communication," *Opt. Exp.*, vol. 24, pp. 30254–30263, 2016.
[12] B. W. Kim and S.-Y. Jung, "Dimmable spatial intensity modulation for visible-light communication: Capacity analysis and practical design," *Current Opt. Photon.*, vol. 2, pp. 532–539, 2018.
[13] S. Kim and S. Y. Jung, "Novel FEC coding scheme for dimmable visible light communication based on the modified Reed–Muller codes," *IEEE Photon. Technol. Lett.*, vol. 23, no. 20, pp. 1514–1516, Oct. 2011.
[14] S. Kim, "Adaptive FEC codes suitable for variable dimming values in visible light communication," *IEEE Photon. Technol. Lett.*, vol. 27, no. 9, pp. 967–969, May 2015.
[15] L. Yin, X. Wu, and H. Haas, "On the performance of non-orthogonal multiple access in visible light communication," in *Proc. IEEE Annu. Int. Symp. Personal, Indoor, Mobile Radio Commun.*, 2015, pp. 1354–1359.
[16] T. Uday, A. Kumar, and L. Natarajan, "MIMO codes for uniform illumination across space and time in VLC with dimming control," *IEEE Photon. J.*, vol. 11, no. 3, pp. 1–21, Jun. 2019.
[17] L. Yin, W. O. Popoola, X. Wu, and H. Haas, "Performance evaluation of non-orthogonal multiple access in visible light communication," *IEEE Trans. Commun.*, vol. 64, no. 12, pp. 5162–5175, Dec. 2016.
[18] S. Rajagopal, R. D. Roberts, and S. K. Lim, "IEEE 802.15.7 visible light communication: Modulation schemes and dimming support," *IEEE Commun. Mag.*, vol. 50, no. 3, pp. 72–82, Mar. 2012.
[19] A. Nuwanpriya, S. Ho, and C. S. Chen, "Indoor MIMO visible light communications: Novel angle diversity receivers for mobile users," *IEEE J. Sel. Areas Commun.*, vol. 33, no. 9, pp. 1780–1792, Sep. 2015.